

# Predicting Plasticization Efficiency from Three-Dimensional Molecular Structure of a Polymer Plasticizer

Maarit Tarvainen,<sup>1,4</sup> Riitta Sutinen,<sup>2</sup> Marja Somppi,<sup>1</sup> Petteri Paronen,<sup>1</sup> and Antti Poso<sup>3</sup>

Received June 18, 2001; accepted September 6, 2001

**Purpose.** In polymeric coatings, plasticizers are used to improve the film-forming characteristic of the polymers. In this study, a computerized method (VolSurf with GRID) was used as a novel tool for the prediction plasticization efficiency ( $\beta$ ) of test compounds, and for determining the critical molecular properties needed for polymer plasticization.

**Methods.** The film-former, starch acetate DS 2.8 (SA), was plasticized with each of 24 tested compounds. A decrease in glass transition temperature of the plasticized free films (determined by differential scanning calorimeter (DSC)) was used as an indicator for  $\beta$ . Partial least squares discriminant analysis was used to correlate the experimental data with the theoretical molecular properties of the plasticizers.

**Results.** A good correlation ( $r^2 = 0.77$ ,  $q^2 = 0.58$ ) between the molecular modeling results and the experimental data demonstrated that  $\beta$  can be predicted from the three-dimensional molecular structure of a compound. Favorable structural properties identified for the potent SA plasticizer were strong hydrogen bonding capacity and a definitive hydrophobic region on the molecule.

**Conclusions.** The VolSurf method is a valuable tool for predicting the plasticization efficiency of a compound. The correlation between experimental and calculated glass transition temperature values verifies that physicochemical properties are primary factors influencing plasticization efficiency of a compound.

**KEY WORDS:** VolSurf; GRID; plasticizer; starch acetate.

## INTRODUCTION

Polymeric films are used in a variety of industrial applications, for example, in pharmaceutical coatings (1), as protective coatings on fruit products (2), and in different types of packaging (3). The main, and usually essential, additives used in these coatings are plasticizers, which change otherwise hard and brittle films to a more pliable and tougher form (4). From a molecular perspective, the plasticizer penetrates into the polymer and increases the free space between the polymer chains by decreasing the cumulative intermolecular

forces along the polymer chains (5). To be compatible, the plasticizer must be miscible with the polymer and must have similar intermolecular forces in the component. In general, the most effective plasticizer closely resembles the polymer it plasticizes. Thus, it can be assumed that the plasticization efficiency is mostly related to the chemical structure of the plasticizer molecule, and the compatibility of the plasticizer with the polymer. However, little is known about the molecular nature of polymer-plasticizer interactions, nor is it entirely known why certain plasticizers are superior to others.

Plasticization generally produces a decreased tensile strength, a lower softening temperature, and a decrease in the glass transition temperature ( $T_g$ ) of the plasticized polymer film (5). The magnitude of these structural changes in the polymer can be used as indicators for the plasticization efficiency of the compound. This evaluation can be made by a number of different semi-empirical tests; for example, by measuring viscosity of the polymer/plasticizer solutions (6), mechanical properties (7),  $T_g$  of the plasticized films (8,9), or by predicting plasticizing efficiency with the aid of the coating components' solubility parameters (10). A weakness of methods based on solubility parameters is that the effects of entropy or the free-volume of amorphous solids are not taken into account. In addition, such variables are extremely sensitive to experimental conditions. Other methods that are generally used in plasticization efficiency assessments are more or less based on trial and error, and reliable predictions cannot be made.

Because  $T_g$  has been demonstrated to be a good indicator of a polymer's structure and chain mobility, and because the purpose of a plasticizer is to increase chain mobility, several researchers have proposed mathematical expressions to describe the compositional dependency of  $T_g$  for a polymer-diluent system (11–13). However, the data needed in these theoretical equations (e.g., "free volumes" or heat capacity of the mixture) are seldom available and often are rather poorly defined. In addition, the specific interactions, that is, hydrogen-bonding formation and charge-transfer, can alter results significantly (14).

Novel computational methods have been developed for the modeling and prediction of physicochemical and pharmacodynamic properties of a compound (15,16). These methods are based on computed interaction fields and multivariate analysis, which correlate three-dimensional (3D) molecular structures with the studied property. For example, blood-brain barrier permeation (17), membrane partitioning of oligopeptides (15), and intestinal absorption (18) all have been successfully predicted with the aid of molecular modeling. Also, the key structural properties responsible for the antiviral activity of some anti-human immunodeficiency virus derivatives have been characterized by chemometric tools (19). Most of these studies were made using a newly developed software package called VolSurf (20). The procedure is fully automated and quite fast, enabling efficient screening of candidates from large collections of compounds.

The aim of this study was to generate a mathematical model for the prediction plasticization efficiency of a compound and to determine the critical molecular properties that are responsible for polymer plasticization. The polymer chosen for this study was a novel pharmaceutical film-former

<sup>1</sup> Department of Pharmaceutics, University of Kuopio, P.O. Box 1627, FIN-70211 Kuopio, Finland.

<sup>2</sup> Centre for Training and Development, University of Kuopio, Kuopio, Finland.

<sup>3</sup> Department of Pharmaceutical Chemistry, University of Kuopio, Kuopio, Finland.

<sup>4</sup> To whom correspondence should be addressed. (e-mail: Maarit.Tarvainen@uku.fi)

**ABBREVIATIONS:**  $\beta$ , plasticization efficiency; LV, latent variable; MW, molecular weight; PC, principal component; PCA, principal component analysis; PLS, partial least squares; SA, potato starch acetate DS 2.8;  $T_g$ , glass transition temperature; 3D, three-dimensional.

potato starch acetate DS 2.8 (SA) (21). Native potato starch is a compound of two polysaccharides, that is, branched amylopectin (80%) and linear amylose (20%) (22). SA forms a strong and tough film structure mainly by dipole interaction forces of the adjacent polyester chains (21). A decrease in  $T_g$  of the plasticized free films (determined by DSC) was used as an indicator for the plasticization efficiency ( $\beta$ ). The correlation of the 3D structural properties of 24 tested compounds and their plasticization efficiency was tested by the VolSurf program with GRID that calculates the molecular interaction fields (23).

## MATERIALS AND METHODS

### Materials

Native potato starch was chemically modified by substituting a portion of the hydroxyl groups on the  $\alpha$ -glucose monomers by acetyl groups in an esterification reaction that resulted in a DS value of 2.8 (24). SA was manufactured by VTT, Chemical Technology, Materials Technology, Rajamäki, Finland.

Most of the compounds investigated in this study were typical plasticizers that are used in pharmaceutical coatings. The dataset included also compounds with promising molecular structures, and compounds having known incompatibles with SA were used as negative controls. The resulting free films were plasticized with each of 24 tested compounds: 2-pyrrolidone;  $\gamma$ -butyrolactone; diethyl phthalate; diethyl succinate; N-hydroxy-succinimide; tributyl phosphate; triethyl phosphate; dimethyl adipate; stearyl alcohol; and trimethyl phosphate (all from Fluka Chemie AG, Buchs, Switzerland); hydantoin; N-methyl-2-pyrrolidone; 2-piperidone; and cyclopentanone (all from Sigma-Aldrich Chemie GmbH, Steinheim, Germany); triethyl citrate and acetyltriethyl citrate (both from Reilly Chemicals, Hautrage, Belgium); triacetin (Unichema Chemie B.V., Gouda, The Netherlands); dibutyl sebacate (Acros Organics, Fair Lawn, New Jersey, USA); glycerol (KEBOLab, Espoo, Finland); mannitol (Merck, Darmstadt, Germany); cetyl alcohol; sorbitol; stearic acid; and xylitol (Ph. Eur.). The structures of the tested compounds are presented in Table I. Chloroform (Labscan Ltd., Dublin, Ireland) was used as a solvent.

### Preparation of Free Films

Free films were prepared by a solvent-cast method. Among several tested solvents, chloroform was selected as having the best solubilizing ability for SA. Initially, the polymer (2% [w/v]) and the plasticizer (40% [w/w] of the total polymer weight) were dissolved in chloroform. The SA-plasticizer solution was cast in a Teflon mold, and the solvent was allowed to evaporate at room temperature for 72 h, resulting in a film with a thickness of 180  $\mu$ m. The dried films were peeled from the mold and were stored at a relative humidity of 57.5% at room temperature for at least 24 h prior to the experiments. The solvent removal from the dried films was assured by an elemental analysis (EA 1110 CHNS-O, ThermoQuest, CE Instruments, Milan, Italy).

The homogeneity of the content and the appearance of the film surface and cross-section were examined by visual observation and scanning electron microscopy (JSM 35 Scan-

ning microscope, Jeol Ltd., Tokyo, Japan), at an accelerating voltage of 15 kV. The film samples were coated with gold before scanning electron microscopy.

### $T_g$ Measurements

The  $T_g$  levels of both unplasticized and plasticized films were measured by a differential scanning calorimeter (7 DSC, Perkin Elmer, Norwalk, Connecticut, USA) with an intra-cooler and nitrogen purge. Each film sample consisted of 8-mg discs that were loaded onto a 50- $\mu$ l aluminum sample pan with a pierced lid to allow for the evaporation of volatile materials. The sample was first heated from 0 °C to 140 °C at a rate of 10 °C/min, and then was cooled back to 0 °C at a rate of 20 °C/min. This step was designed to remove moderately bound moisture and solvent residues so that the endotherm would not obscure the glass transition. The sample then was reheated at a rate of 10 °C/min until the  $T_g$  had passed. The  $T_g$  for each film type was determined from the midpoint of a small endothermic rise of the pretransition and post-transition baselines using three parallel thermograms. The method was similar to the one described by Okhamafe and York (25). The  $\beta$  of the compound was stated as a difference between the  $T_g$  of a plasticized SA film and the  $T_g$  of an unplasticized SA film (134 °C).

### Computational Approach

Molecular structures were created by the sketch tool Sybyl (version 6.6) (Tripon Inc., St. Louis, Missouri), and further minimized using the MMFF94s force field. All chemicals were modeled in their neutral form. To describe the 3D molecular field of the compound, the GRID force field was used (GRID program, version 18) (26). Four probes (i.e., hydrophilic, hydrophobic, carboxyl oxygen, and amide) were used to characterize interaction sites around target molecules. These probes, with eight different energy levels, were chosen to simulate polymer-plasticizer interactions.

3D molecular field maps were transformed into 88 scalar descriptors by VolSurf (version 2.0.6). These molecular descriptors had clear chemical meanings, referring to, for example, molecular volume (V), shape (S), surface rugosity (R) (which is calculated from V/S ratio), molecular weight (MW), size of the hydrophilic (W) and hydrophobic (D) regions, and hydrogen-bonding properties (HB). A critical packing parameter (CP) described the ratio between the D and W part of a molecule. Other useful descriptors were integrity moments, measuring the distribution between a molecule's center of mass and the position of surrounding hydrophilic (TW) and surrounding hydrophobic (ID) regions, and capacity factors (CW) representing the ratio between the hydrophilic regions and the molecular surface. Also, the distances between the best three local minima of interaction energies (D12, D13, and D23) were determined by a water probe and were calculated by VolSurf. The number (1–8) after the abbreviation of the specific descriptor describes the energy level used for statistical analysis and, thus, the strength of the interaction energy between molecule and probe. A more detailed representation of VolSurf descriptors has been presented by Cruciani *et al.* (20).

Chemometric tools, principal component analysis (PCA), and partial least squares (PLS) analysis were used to compile the information obtained from VolSurf. PCA sum-

**Table I.** The 15 (1–15) Compounds Used in the First Training Set Model, the 9 (16–24) Compounds Used for External Prediction, and Measured ( $\beta$ ) and Calculated Plasticization Efficiencies Using Datasets of Either 15 ( $\beta_1$ ) or 24 ( $\beta_2$ ) Compounds

Plasticizer	Structure	$\beta$ ( $^{\circ}\text{C}$ ) (mean $\pm$ SD)	$\beta_1/\beta_2$ ( $^{\circ}\text{C}$ )	Plasticizer	Structure	$\beta$ ( $^{\circ}\text{C}$ ) (mean $\pm$ SD)	$\beta_1/\beta_2$ ( $^{\circ}\text{C}$ )
[1] Sorbitol		$17 \pm 2$	10/2	[13] 2-pyrrolidone		$-73 \pm 2$	-40/-41
[2] Stearic acid	$\text{CH}_3(\text{CH}_2)_{16}\text{COOH}$	$3 \pm 5$	0/7	[14] Triacetin		$-76 \pm 1$	-68/-75
[3] Cetyl alcohol	$\text{CH}_3(\text{CH}_2)_{14}\text{CH}_2\text{OH}$	$0 \pm 0$	-9/-6	[15] Tributyl phosphate		$-77 \pm 4$	-56/-54
[4] Xylitol		$-17 \pm 2$	-4/-4	[16] Stearyl alcohol	$\text{CH}_3(\text{CH}_2)_{16}\text{CH}_2\text{OH}$	$13 \pm 3$	-2/7
[5] Hydantoin		$-25 \pm 1$	-37/-36	[17] Dibutyl sebacate	$\text{CH}_3(\text{CH}_2)_3\text{COO}-$ $(\text{CH}_2)_8\text{COO}-$ $(\text{CH}_2)_3\text{CH}_3$	$-9 \pm 1$	-35/-22
[6] Butyrolactone		$-31 \pm 0$	-52/-52	[18] Glycerol		$-11 \pm 1$	-23/-17
[7] N-hydroxy-succinimide		$-38 \pm 3$	-37/-40	[19] Mannitol		$-16 \pm 3$	3/-5
[8] N-methyl-2-pyrrolidone		$-45 \pm 2$	-42/-43	[20] Cyclopentanone		$-31 \pm 1$	-46/-47
[9] Diethyl succinate		$-50 \pm 1$	-63/-65	[21] Trimethyl phosphate		$-47 \pm 3$	-61/-57
[10] Acetyltriethyl citrate		$-55 \pm 1$	-67/-73	[22] 2-piperidone		$-67 \pm 3$	-42/-44
[11] Triethyl phosphate		$-59 \pm 2$	-65/-60	[23] Dimethyl adipate		$-67 \pm 1$	-55/-50
[12] Diethyl phthalate		$-70 \pm 7$	-65/-64	[24] Triethyl citrate		$-70 \pm 3$	-54/-62

marized information contained in the X-matrix (i.e., the molecular properties of the tested compounds) by a few principal components (PCs). PCA also was used to find "outliers" that differ remarkably from other compounds. PLS analysis, on the other hand, was used to correlate the experimental data (Y-matrix; the plasticization efficiency of the compound) with

the X-matrix. In PLS modeling, latent variables (LVs), which are quite equivalent to the PC in PCA, were used as linear combinations of the original X-variables. The number of significant LVs to include was determined by cross-validation. PLS modeling gives valuable information about molecular properties that are critical for efficient plasticization behavior.

ior. Two PLS models were created; compounds 1–15 were used for the prediction of the plasticization efficiencies of compounds 16–24, and the second model considered all 24 compounds (Table I). Fractional factorial design was used to remove irrelevant descriptors that did not have any relationship to the plasticization efficiency, and, in this way, the predictive ability of the PLS model could be improved. The quality (i.e., the explanatory power,  $r^2$ ) and the predictive ability (i.e.,  $q^2$ ) of the PLS model were evaluated by cross-validation. This validation was done by randomly dividing the compounds into five groups, and then models were built by keeping one of these groups out of the analysis.

## RESULTS AND DISCUSSION

### Appearance of the Films and Experimental Plasticization Efficiency

Elemental analysis showed that there was some unavoidable solvent retention in the unplasticized SA films. However, there was no clear evidence of solvent residue in the plasticized SA films. The reason for the lower solvent retention in plasticized SA films, compared to plain SA films, might be due to the plasticizer replacing the solvent molecule in the polymer (27). Thus, the method used in free film preparation was considered to be suitable for evaluating the plasticization efficiency of the tested compounds on SA.

A poor plasticization efficiency of the compound on SA was noticed as a hard and brittle film structure. Compounds incompatible with SA formed white and uneven films (an SA-glycerol film as an example, Fig. 1A), whereas SA films with efficient plasticizers were transparent and smooth (an SA-2-pyrrolidone film as an example, Fig. 1B).

Glass transitions of the films determined by DSC were apparent, and the mean standard deviation in  $T_g$  measurements was lower than 2 °C. The most efficient plasticizer depressed  $T_g$  by 77 °C ( $\beta$ ; Table I). The compounds that were most incompatible with SA, on the other hand, raised the  $T_g$ , which can be described as an antiplasticizing effect (28). In general, films were clear and transparent when the decrease in the  $T_g$  was higher than 30 °C.

### PCA

The PCA model having the first two PCs could not divide the compounds into two separate groups, the poor plasticizers (i.e., a decrease in  $T_g$  lower than 30 °C) and the efficient plasticizers (i.e., the decrease in  $T_g$  higher than 30 °C) (Fig. 2). However, efficient plasticizers grouped near the minima of PC 1, whereas poorer plasticizers, except for hydantoin, dibutyl sebacate, and glycerol, had higher absolute values for PC 1. Thus, the generated PCA model satisfactorily discriminated compounds by their 3D structure, even if the applied training model was quite small. In addition, no outliers were found by PCA.

### PLS Analysis

Initially, the quality and predictive power of the PLS model was tested by using 15 compounds in the training set for the prediction of the plasticization efficiency for the other nine compounds (Table I). The relationship between experimental  $\beta$  and calculated  $\beta_1$  gave an  $r^2$  of 0.71 with a  $q^2$  of 0.41.

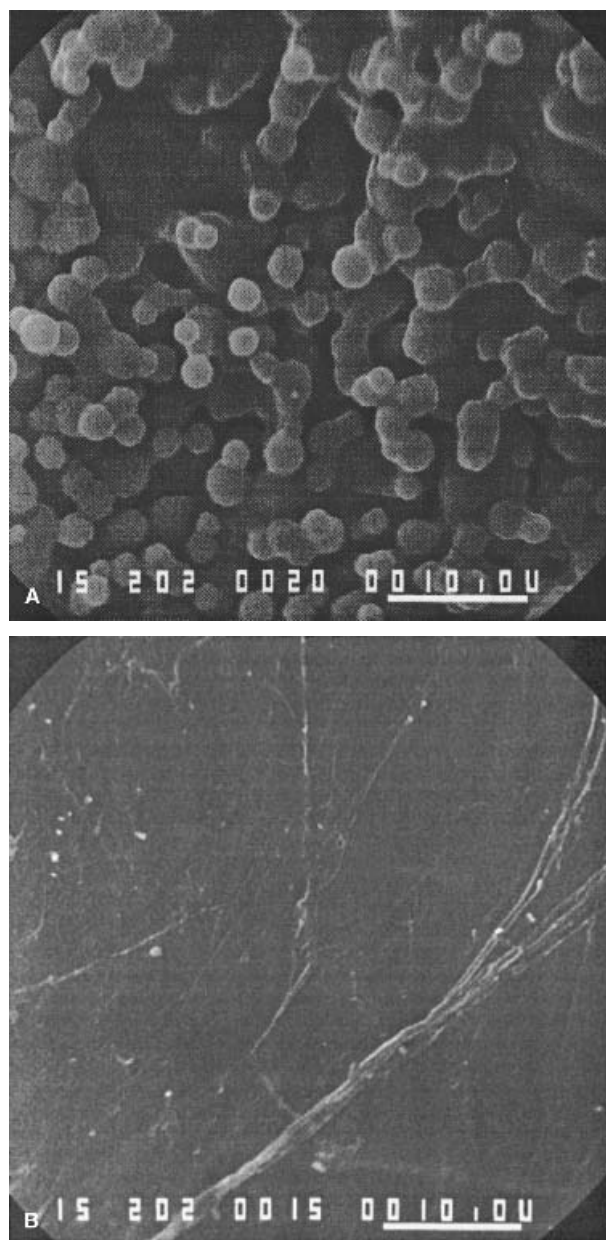


**Fig. 1.** Scanning electron micrographs of starch acetate (SA) films, plasticized with 40% glycerol (A) and 2-pyrrolidone (B) (bar = 10  $\mu\text{m}$ ).

Even with this rather small training set, the model satisfactorily predicted the plasticizing efficiency of the compounds, and, thus, the final model using the entire dataset (24 compounds) could be built. The predictive power for  $\beta_2$  of the final model improved remarkably, giving a  $q^2$  value of 0.58, and also the  $r^2$  was higher (0.77), compared to the first model (Fig. 3, Table I). The standard deviation of the first model's predictive ability was 18 °C, which indicates a satisfactory accuracy in distinguishing compounds as poor, moderate, and efficient SA plasticizers. The first LV of PLS distinguished between the poor plasticizers (the decrease in  $T_g$  lower than 30 °C) and the efficient plasticizers (the decrease in  $T_g$  higher than 30 °C) (Fig. 4).

After the quality of the model was demonstrated, our second area of interest was to determine the factors affecting

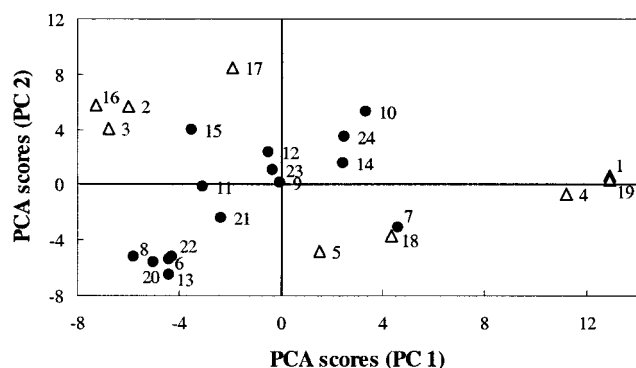


**Fig. 2.** PCA score plot with two PCs (PC 1 vs. PC 2) for the compounds reported in Table I. Compounds that decreased  $T_g$  less than 30 °C ( $\Delta$ ) and compounds that decreased  $T_g$  more than 30 °C ( $\bullet$ ) are shown.

plasticization efficiency. The fractional factorial design procedure decreased the number of VolSurf descriptors from 88 to 41. These 41 relevant descriptors could be summarized by two LVs, which were found to be significant by a cross-validation technique. Because efficient plasticizers had a large negative value for  $\beta$ , the favorable properties for these compounds were presented by descriptors having negative values in both LVs. These advantageous VolSurf descriptors of the model and, also, the disadvantageous ones for plasticization efficiency, are presented as negative and positive regression coefficients, respectively, in Fig. 5.

Surprisingly, PLS analysis showed that the SA plasticizer molecule should not have large hydrophobic regions (descriptors D1–D6 in Fig. 5), even if the polysaccharide studied has almost all hydroxyl groups substituted by the D acetyl groups. For example, stearic acid, cetyl alcohol, and stearyl alcohol were too D to be miscible in SA, and thus no plasticization effect was noticed. Also, the longer hydrocarbon chain of dibutyl sebacate impaired the plasticization efficiency, compared to that of dimethyl adipate. However, in the case of phosphate derivatives the plasticization efficiency improved when the side chain was increased from methyl to butyl. Thus, some hydrophobicity is beneficial for the plasticization ability. In addition, dominating hydrophilic regions proved to be disadvantageous for the plasticization efficiency, and only the highest energy level with the amide probe (W8) gave a negative PLS coefficient. As a result, sorbitol, xylitol, glycerol, and

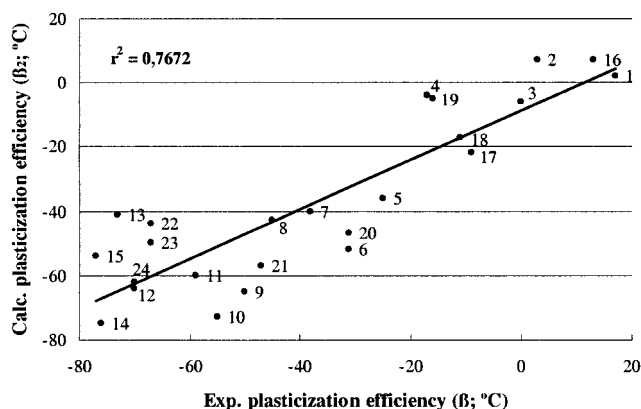


**Fig. 3.** Plot of experimental  $\beta$  vs. calculated plasticization efficiency ( $\beta_2$ ) for the compounds reported in Table I.

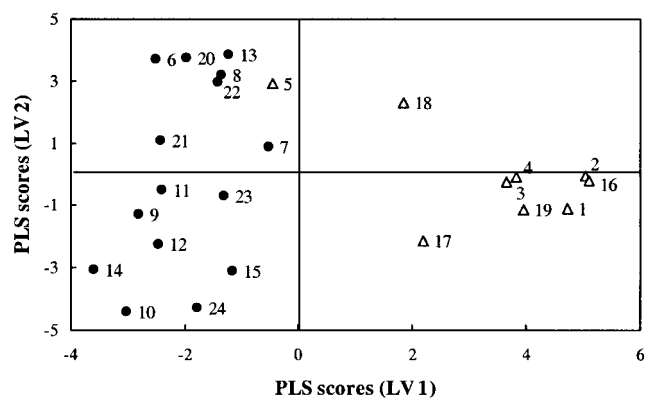


**Fig. 4.** PLS score plot with two LVs (LV 1 vs. LV 2) for the compounds reported in Table I. ( $\Delta$ ) represent compounds that decreased  $T_g$  less than 30 °C, and ( $\bullet$ ) represent compounds that decreased  $T_g$  more than 30 °C.

mannitol, for example, were too hydrophilic as SA plasticizers. Thus, it is impossible to predict plasticization efficiency directly from the aqueous solubility of the plasticizer, as tributyl phosphate and dibutyl sebacate, for example, both have low aqueous solubilities, although the former is much more efficient as an SA plasticizer. As with aqueous solubility, solubility parameters of the plasticizers also proved to be useless in plasticization efficiency predictions. Triacetin was a much more effective SA plasticizer when compared to dibutyl sebacate, for example, even if the solubility parameters for both compounds were similar (triacetin, 18.0–20.2 MPa<sup>1/2</sup>; dibutyl sebacate, 15.7–18.8 MPa<sup>1/2</sup> (29)).

The results indicated that a potent SA plasticizer should have both hydrophilic and hydrophobic regions and, in addition, a definitive concentration of a hydrophobic region in only one part of the molecular surface (ID5, ID6) and a clear attractive region determined by the hydrophilic probe (D23) (Fig. 5). As a result, simple log P values (calculated by ACD/log P DB, version 4.56, Toronto, Canada) could not be used for the plasticization efficiency predictions due to the poor correlation ( $r^2 = 0.02$ ) between log P and  $\beta$ . The strong negative PLS coefficients for hydrogen-bonding capacity with the

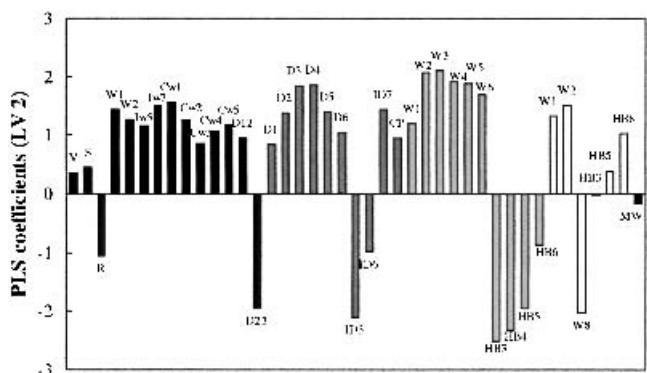


**Fig. 5.** PLS coefficient plot for the correlation of VolSurf descriptors with plasticization efficiency ( $\beta$ ). Descriptors were defined by hydrophilic (black bars), hydrophobic (dark gray bars), carboxyl (light gray bars), and amide (white bars) probes. The long bar represents a strong relationship between the descriptor and the plasticization efficiency. Abbreviations for the VolSurf descriptors are given in the Materials and Methods section.

carboxyl probe (HB3-HB6) meant that for a compound to be efficient in SA plasticization, there should be hydrogen-bonding acceptor abilities (Fig. 5). Thus, carbonyl oxygens of esters (e.g., triethyl citrate and dimethyl adipate) are apparently able to interact with the remaining hydroxyl groups ( $DS, \approx 0.2$ ) of SA. Also, the accessibility of these carbonyl oxygens is important, such that there are no bulky side groups to reduce the possibilities for interactions (9). However, hydrogen bonding between the plasticizer and the polymer that is too strong may yield a cross-linking network, with a resulting fall in a polymer chain's mobility and a rise in  $T_g$  (28). The rather weak ability of SA to accept hydrogen has been noticed as insolubility in alcoholic solvents. VolSurf analysis demonstrated that the average molecular polarizability is meaningless when considering the plasticization efficiency of the compound.

Besides the parameters describing different interactions between a molecule and the selected probes (and the polymer), the shape and size of the compound seemed to be meaningful when considering its plasticization efficiency (Fig. 5). An SA plasticizer should have small rugosity, and PLS analysis also showed that there is a correlation between the MW and the plasticization efficiency of the compound. However, this could only be seen when the decrease in  $T_g$  was higher than 20 °C and the MW was between 86 and 250 (Fig. 6). The only exceptions (which were excluded from Fig. 6) were 2-pyrrolidone and 2-piperidone, which showed better plasticization efficiency than could be predicted from their MWs. These compounds did not fit satisfactorily in the PLS model either (Table I, Fig. 3). A possible reason for the poor predictability for 2-pyrrolidone and 2-piperidone could be explained by their plasticization mechanisms, which may differ from those of other tested plasticizers. As the sampling was rather limited in this study, the PLS model could not find the molecular properties resulting in this unpredictably strong plasticization efficiency. Another reason for the poor predictability of the generated model for 2-pyrrolidone and 2-piperidone could be the higher compatibility limit (28) of these compounds with SA compared to that of other tested plasticizers.

As with MW, the effect of a single molecular property is often parabolic, that is, the single property has an optimum value that is favorable in polymer plasticization. When the above-mentioned conditions were fulfilled, the efficient plasticizer (e.g., triethyl citrate and tributyl phosphate in the case of SA) was able to diffuse and strongly interact with active

groups in the polymer. As with polymer blends, this compatibility (i.e., miscibility) is influenced by both the energetic interactions and conformational rearrangements in the neighborhood of the hetero-contacts (14). However, a closer examination is needed to study what forces exist between the plasticizer and the polymer. The interaction forces can occur through hydrogen bonding or through electrostatic or dispersion forces (9). In the present study, only the sum of these interaction forces could be detected by using the  $T_g$  of the plasticized film as an indicator for the capacity of the polymer-plasticizer interaction. In addition, the quality and predictability of the developed VolSurf model was only tested at one plasticizer concentration. Thus, the type of plasticization, whether it is molecular or structural (30), or the compatibility limit in the polymer for the single compound could not be detected in this study. However, the use of a single concentration of plasticizer for the prediction of its plasticization efficiency is adequate to discriminate between poor, moderate, and efficient plasticizers.

## CONCLUSIONS

The VolSurf method is a valuable tool for predicting the plasticization efficiency of a compound, because there is a clear correlation between the 3D structure of a compound and its plasticization efficiency (i.e., interactions between the polymer and the plasticizer). The correlation between experimental and calculated  $T_g$  values verifies that physicochemical properties are primary factors influencing the plasticization efficiency of a compound. In the case of the tested polymer, starch acetate, successful polymer plasticizers were found to have a strong hydrogen-bonding capacity and a definitive D region on the molecule. Although the experimental data have been presented for only one polymer in this article, this chemometric method can be broadly applied in the polymeric science of other fields, for example, in the screening of compatible additives or solvents for different polymer applications, where the interaction of these two compounds is responsible for the matter studied. Moreover, the modeling of the polymer itself is not needed. Thus, this approach can reduce the need for traditional time-consuming and expensive preformulation, and at the same time, it is possible to receive valuable information from different structure-activity relationships.

## ACKNOWLEDGMENTS

The authors are grateful to M.Sc. Erik Wallén and Mrs. Tiina Koivunen for elemental analysis. We are also grateful to PhLic Soili Peltonen and PhLic Hannu Mikkonen for their skillful guidance during this study. The financial support from TEKES (the Technology Development Centre in Finland) is gratefully acknowledged. This study was also supported by grants from the Pharmacal Foundation and The Kuopio University Foundation.

## REFERENCES

1. J. E. Hogan. Film-coating materials and their properties. In G. Cole (ed.), *Pharmaceutical Coating Technology*, Taylor & Francis Ltd, London, United Kingdom, 1995 pp. 6–52.
2. M. A. García, M. N. Martino, and N. E. Zartitzky. Plasticized starch-based coatings to improve strawberry (*Fragaria × Ana-*

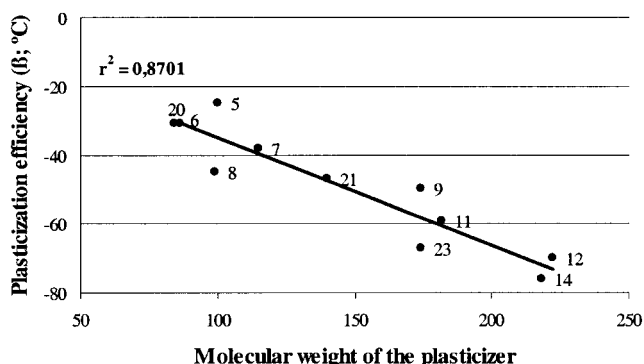


Fig. 6. MW of the compound vs. plasticization efficiency ( $\beta$ ; °C) (data in Table I).

- nassa) quality and stability. *J. Agric. Food Chem.* **46**:3758–3767 (1998).
3. F. Debeaufort and A. Voilley. Methylcellulose-based edible films and coatings: 2. Mechanical and thermal properties as a function of plasticizer content. *J. Agric. Food Chem.* **45**:685–689 (1997).
  4. F. V. Billmeyer. Plastics technology. In F. V. Billmeyer (ed.), *Textbook of Polymer Science, 2nd ed.*, John Wiley & Sons, New York, 1971 pp. 491–512.
  5. G. S. Banker. Film coating theory and practice. *J. Pharm. Sci.* **55**:81–89 (1966).
  6. P. S. Shah and J. L. Zatz. Plasticization of cellulose esters used in the coating of sustained release solid dosage forms. *Drug Dev. Ind. Pharm.* **18**:1759–1772 (1992).
  7. S.-Y. Lin, C.-J. Lee, and Y.-Y. Lin. The effect of plasticizers on compatibility, mechanical properties, and adhesion strength of drug-free Eudragit E films. *Pharm. Res.* **8**:1137–1143 (1991).
  8. A. Schade, T. Niwa, H. Takeuchi, T. Hino, and Y. Kawashima. Aqueous colloidal polymer dispersions of biodegradable DL-lactide/glycolide copolymer as basis for latex films: a new approach for the development of biodegradable depot system. *Int. J. Pharm.* **117**:209–217 (1995).
  9. J. C. Gutiérrez-Rocca and J. W. McGinity. Influence of water soluble and insoluble plasticizers on the physical and mechanical properties of acrylic resin copolymers. *Int. J. Pharm.* **103**:293–301 (1994).
  10. B. C. Hancock, P. York, and R. C. Rowe. The use of solubility parameters in pharmaceutical dosage form design. *Int. J. Pharm.* **148**:1–21 (1997).
  11. F. N. Kelley and F. Bueche. Viscosity and glass temperature relations for polymer-diluent systems. *J. Polym. Sci.* **L**:549–556 (1961).
  12. M. C. Righetti, G. Ajroldi, and G. Pezzin. The glass transition temperature of polymer-diluent systems. *Polymer* **33**:4779–4785 (1992).
  13. B. C. Hancock and G. Zografi. The relationship between the glass transition temperature and the water content of amorphous pharmaceutical solids. *Pharm. Res.* **11**:471–477 (1994).
  14. H. A. Schneider. Glass transition behaviour of compatible polymer blends. *Polymer* **30**:771–779 (1989).
  15. L. H. Alifrangis, I. T. Christensen, A. Berglund, M. Sandberg, L. Hovgaard, and S. Frokjaer. Structure-property model for membrane partitioning of oligopeptides. *J. Med. Chem.* **43**:103–113 (2000).
  16. G. Cruciani, M. Pastor, and W. Guba. VolSurf: a new tool for the pharmacokinetic optimization of lead compounds. *Eur. J. Pharm. Sci.* **11**(Suppl.):29–39 (2000).
  17. P. Crivori, G. Cruciani, P.-A. Carrupt, and B. Testa. Predicting blood-brain barrier permeation from three-dimensional molecular structure. *J. Med. Chem.* **43**:2204–2216 (2000).
  18. U. Norinder, T. Österberg, and P. Artursson. Theoretical calculation and prediction of intestinal absorption of drugs in humans using MolSurf parametrization and PLS statistics. *Eur. J. Pharm. Sci.* **8**:49–56 (1999).
  19. E. Filippini, G. Cruciani, O. Tabarrini, V. Cecchetti, and A. Fravolini. QSAR study and VolSurf characterization of anti-HIV quinolone library. *J. Comput. Aided Mol. Design* **15**:203–217 (2001).
  20. G. Cruciani, P. Crivori, P.-A. Carrupt, and B. Testa. Molecular fields in quantitative structure-permeation relationships: the VolSurf approach. *J. Mol. Struct. (Theochem)* **503**:17–30 (2000).
  21. M. Ahola, P. Tiitonen, R. Sutinen, S. Peltonen, and P. Paronen. Novel polymer – starch acetate – for tablet coating. *Eur. J. Pharm. Sci.* **8**(Suppl.):38–39 (1999).
  22. A. H. Young. Fractionation of starch. In R. L. Whistler, J. N. Bemiller, and E. F. Paschall (eds.), *Starch: Chemistry and Technology, 2nd ed.*, Academic Press, San Diego, California, 1984 pp. 249–283.
  23. P. J. Goodford. A computational procedure for determining energetically favorable binding sites on biologically important macromolecules. *J. Med. Chem.* **28**:849–857 (1985).
  24. T. P. Paronen, S. Peltonen, A. Urtti, and L. Nakari. Starch acetate composition with modifiable properties, method for preparation and usage thereof. US Patent 5667803 (1997).
  25. A. O. Okhamafe and P. York. Studies of interaction phenomena in aqueous-based film coatings containing soluble additives using thermal analysis techniques. *J. Pharm. Sci.* **77**:438–443 (1988).
  26. Molecular Discovery Limited. GRID software Linux-version, Molecular Discovery Limited, Oxford, England (2000).
  27. J. C. Gutiérrez-Rocca and J. W. McGinity. Influence of aging on the physical-mechanical properties of acrylic resin films cast from aqueous dispersions and organic solutions. *Drug Dev. Ind. Pharm.* **19**:315–332 (1993).
  28. A. O. Okhamafe and P. York. Thermal characterization of drug/polymer and excipient/polymer interactions in some film coating formulation. *J. Pharm. Pharmacol.* **41**:1–6 (1989).
  29. T. A. Wheatley and C. R. Steuernagel. Latex emulsions for controlled drug delivery. In J. W. McGinity (ed.), *Aqueous Polymeric Coatings for Pharmaceutical Dosage Forms, 2nd ed.*, Marcel Dekker, Inc., New York, 1997 pp. 1–54.
  30. B. Garnaik and S. Sivaram. Study of polymer-plasticizer interaction by <sup>13</sup>C CP/MAS NMR spectroscopy: Poly(vinyl chloride)-Bis(2-ethylhexyl) phthalate system. *Macromolecules* **29**:185–190 (1996).